- Technical Paper -

A CRACK DETECTION METHOD FOR CONCRETE INFRASTRUCTURES BASED ON IMAGE PROCESSING TECHNIQUE AND GENETIC ALGORITHM

Cuong Nguyen KIM*[1], Kei KAWAMURA*[2], Amir TARIGHAT*[3], Hideaki NAKAMURA *[4]

ABSTRACT

This paper presents a crack detection method based on genetic algorithm to optimize the parameters of image processing technique (IPT). Morphological mathematic is applied to the pre-processing step in order to smooth the original image. Next, the global binarization and dilation-thinning operation is used for segmentation and noise removal. Moreover, the experimental results of the proposed method compared with other methods for concrete infrastructure surface images under various complex photometric conditions validate the reasonable accuracy in practical applications.

Keywords: genetic algorithm, image processing, crack detection, concrete infrastructure

1. INTRODUCTION

Many concrete components of existing infrastructure systems such as bridges, and tunnels have suffered from various geologic, loading and environmental conditions cause to cracks which make influent to quality of operations. Therefore, the condition assessment of the existing infrastructures is an important task not only for warming against deterioration but also for guaranteeing soon maintenance. Concrete cracks are important indicators reflecting the safety of infrastructure. The automatic crack detection of infrastructure surface is typically usage of non-destructive testing technique. This technique can be implemented using some of different image data captured from ultrasonic device, infrared and thermal device, laser scanning, and commonly digital cameras.

Due to availability of high accuracy, simplicity and low-cost, the digital camera image based crack detection has rapidly increased in recent years. In addition, there are main three approaches based on threshold technique (Ito et al. 2002 [1]; Miyamoto et al. [2]; Fujita el al [3]), edge detection technique (Yu et al. 2007 [4]), and model-based approach (Ukai 2000 [5]; Yamaguchi and Hashimoto 2010 [6]; Zhu et al. 2011 [7]). The crucial drawback of the threshold-technique approach is questionable.

It is difficult to choose a suitable threshold value for extracting crack pixels in various complex back ground images. This method typically selects a threshold based on prior knowledge. If the threshold value is too large the crack pixels is lost. The threshold value is too small to appear much noise pixels. Therefore, the threshold value has to search an optimal value based on convolution algorithms.

Abdel-Qader et al. [8] compared with some of edge detection algorithms and found Haar Wavelet Transform (HWT) method to be the most reliable of them. However, comparing other methods [3] [9], HWT method didn't yield the high accuracy for automatic crack detection based on edge detection technique. According to [10], the accuracy of model based approach is relied on user input to initialize the seed pixels. Consequently, hairline cracks may not be detection because users may be unable to identify the seed pixels. To achieve the accuracy of automatic crack detection, the parameters of image processing technique have to find the optimal values based on convolution algorithms.

In recently years, Kawamura et al. [11] proposed interactive genetic algorithm is applied to adjust the image processing parameters. It is developed to extract crack pattern effectively. Nishinkawa et al. [12] designed System for Automatic Construction of Image Filter (SACIF) based on a genetic program to detect cracks on concrete structures.

The main aim of this paper is to combine genetic algorithms (GA) adjusted optimized parameters and IPTs which are capable of detecting the cracks of the various complex surface images of the concrete infrastructures.

2. PROPOSED METHOD

2.1 Overview

In practical applications, surface images of concrete infrastructures are captured under various conditions. Raw original images include in useless

*1 Ph.D. Candidate, Graduate school of Science & Engineering, Yamaguchi University, JCI Member
*2 Associate Prof. Graduate School of Science & Technology for Innovation, Yamaguchi University, JCI Member
*3 Associate Prof, Shahid Rajaee Teacher Training University, Teheran, Iran.
*4 Prof. Graduate School of Science & Technology for Innovation , Yamaguchi University, JCI Member

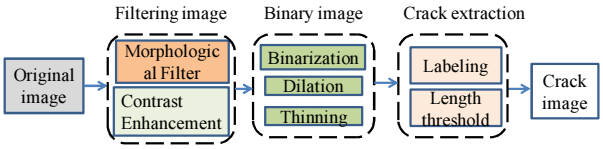

Fig.1 Image processing procedure

information called noises due to uneven illumination, low contrast, and other distortions. Therefore, pre-processing step is substantial to smooth the original image. Many researchers use image filters such as wavelet transform [8], Laplace Sobel transformation [4], mathematic morphology [13][14][15], and median filter [3].

In this paper, morphological operations are applied to smooth and remove the noises of the original images. After that, histogram equalization is applied to enhance the contrast before binarization. Next, dilation-thinning transform is used to sharp the crack pixels and remove noise. Finally, length threshold is adopted to clean noise significantly.

Moreover, authors use GA to search the optimized parameter values of the IPT. The proposed method compares with [9][16] methods.

2.2 Image processing technique

Fig.1 shows the image processing procedure included in three main parts. Namely, there are filtering image part, binary image part, and crack extraction part. Therein, filter image part comprises of morphological filter transform and contrast enhancement. The second part consists of binarization, and dilation-thinning transformation. The final part comprises of labeling and length threshold. The detailed steps as follow:

(1) Morphological filter

The morphology filter consists of opening of closing operation on gray-scale image with a predefined structuring element as the following equation:

$$M = \max([(I \bullet S) \circ S], I) - I \qquad (1)$$

Where M means the smooth image after morphological image processing, S is a structuring element, and 'o' and '•' are the morphological opening and closing operators. I is a gray-scale image converting from the corresponded original image. Additionally Opening transform includes dilation of erosion. Closing is an inverse operator of the opening as the following Eqs. (2) and (3):

$$(F \circ S) = (F \Theta S) \oplus S \qquad (2)$$

$$(F \bullet S) = (F \oplus S) \Theta S \qquad (3)$$

Given grayscale image $F_{(x,y)}$ and structuring element $S_{(u,v)}$, the dilation and erosion operations are defined by:

$$(F \oplus S)_{(x,y)} = \max_{u,v}(F_{(x-u,y-v)} + S_{(u,v)}) \qquad (4)$$

$$(F \Theta S)_{(x,y)} = \min_{u,v}(F_{(x-u,y-v)} - S_{(u,v)}) \qquad (5)$$

The purpose of this part is firstly to smooth image as well as eliminate noises and shading and then make the sharpness of crack edge. For an example, Fig.2 (b) shows the result of smooth image M.

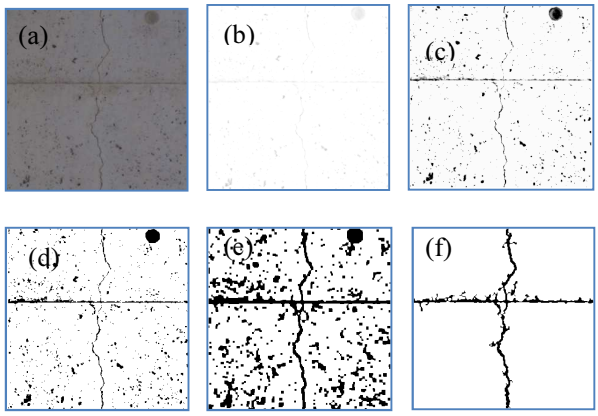

Fig 2. The illustrative results of image processing procedure. (a): Original image; (b): Morphological filter; (c): Contrast enhancement; (d):Binarization; (e): Dilation-thinning transform; (f): Final crack image.

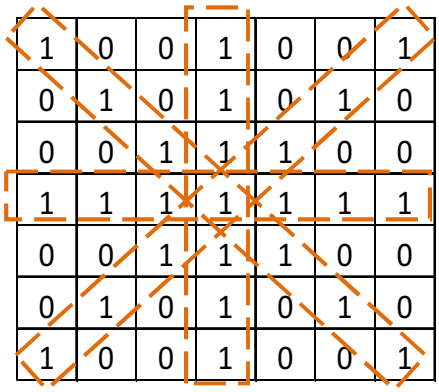

Fig.3 A designed structuring element with combination of four directions and (7x7) pixels size of line-type

(2) Structuring element design

Because the shape of crack is irregular elongation, the shape of the structuring element of line-type is adopted. To retrieve fully crack information in the various directions, combination line types of four directions into the structuring element such as $\{0^0, 45^0, 90^0, 135^0\}$ or six directions $\{0^0, 30^0, 60^0, 90^0, 120^0, 150^0\}$. In this study, the former type is used to reduce computational volume, as shows in Fig.3.

(3) Contrast Enhancement

Surface images of civil infrastructure are the typical dark environmental condition, narrow contrast. The intensity of crack pixels and background pixels is not much difference. Therefore before binarization is applied a histogram of the raw image is equalized to sharpen crack pixel as the following equation:

$$q_k = \sum_{i=0}^{k} \frac{n_i}{n} \quad k = 0,1,2,..L-1 \qquad (6)$$

$$I_k(\text{out}) = (I_{max} - I_{min}) \times q_k(\text{in}) + I_{min}$$

Where, n_i: is number of pixels that have i^{th} gray-scale

value. n: the number of pixels; k: the input gray-scale level. L: the maximum gray-scale level (255).
q_k: acquired normalized histogram. I_{max} and I_{min} are respective to the maximum and minimum intensities of the original image. I_k(out) is the new gray-scale intensity of the input pixel having q_k(in). As a result, Fig2.(c) shows crack enhancement after morphology filter is applied to smooth the original image.

(4) Binarization

As shown in Eq. (7), the purpose of binarization is to segment gray-scale image into binary image. The binary image only has two values 255 (white pixel is background) and 0 (black pixel is crack or noise).

$$P(i)=\begin{cases}0 \ if \ I(x_i)>255-T \\ 255 \ \ otherwise\end{cases} \quad (7)$$

Where T is a threshold value of the binarization (binary), it is necessary to find out an optimal value. $P(i)$ is the i^{th} pixel value after binarization step.

(5) Dilation

The aim of a dilation operation is to connect crack fragments meanwhile noises are separated from the cracks. Therefore it results in the reduction of loss pixel. However, widths of crack pixels increase along with the crack shape. The size of structuring element of the dilation operation is considered as an adjusted parameter to optimized value by GA. In this paper, the shape of structuring element is predefined in "square" type. The rule of the dilation operation is if any pixel in the input neighborhood is "1", the output pixel is "1". Otherwise, the output pixel is "0".

(6) Thinning

Thinning to a binary image is a morphology operator used to remove noise surrounding crack pixels. [17].The purpose of this step is to prune branches from the crack shape as well as reduce noises after dilation operator is performed. Fig.2 (e) shows the image processing result of dilation and thinning transform.

(7) Labeling and length threshold

After thinning, the pixel values of the image are presented by the 0s or 255s. Consequently, the labeling step is to connect neighboring components as a single object with the same number.

Hence, a single object can be a crack object or a noise object. In effect, the length threshold step is performed to improve noise removal. The shape of connection component after the labeling step is classified by the following equation:

$$P'^{(i)}=\begin{cases}255 \ if \ \dfrac{Max\left(R_{xi},\ R_{yi}\right)^2}{S_i}<\mathrm{T}' \\ 0 \qquad otherwise\end{cases} \quad (8)$$

Where T' is a threshold value of the i^{th} label length to distinguish between a crack object and a noise object. S_i is the total number of pixels of the i^{th} label. R_{xi}, and R_{yi} are the number of pixels of the i^{th} label in the horizontal and vertical directions, respectively.

2.3 Application of GA to the image processing parameters optimization

Fig. 4 A represented chromosome for solution candidates

Table 1 Properties of parameter

Variable	Range	Steps	Bits
fs	[1 127]	2	6
bi	[0 255]	1	8
di	[1 31]	0.5	4
li	[0 32.5]	0.5	6

The GA, proposed in the 1970s, is one of the optimization algorithms base on inspiring biologically behavior for solving an implicit or uncertainty problem. No losing generality, Assumption that a solution candidate is represented by a chromosome of an individual in the population. The chromosome contains information in term of tuned parameter values which is encoded by binary strings. Weak individuals will be removed as well as elite members would keep in the next generation. The quality of population is improved by performing genetic operations in each generation. The GA is applied to search optimal values of the image processing parameters (IPPs) because its advantage is to avoid local optimization as other conventionally evolutional algorithms.

(1) Represented chromosome Design for solution candidates

Firstly, the IPPs are combined to create an individual in a population. Secondly, each individual is represented by a chromosome encoded to a binary string, as shown in Fig 4.

Namely, the size of structuring element (fs) is assigned by 6 bits, the threshold value of binarization (bi) is expressed by 8 bits, dilation transform parameter (di) is expressed by 4 bits, and the linear degree is expressed by 6 bits (li). Table 1 shows some parameter values. Therein, the ranges of the parameter values are based on the preliminary experiments.

(2) Genetic algorithm

Fig.5 shows an operated mechanism of GA including into the crucial three stages. Namely, they consist of the initial population generation, fitness evaluation of each individual in the current population, and evolution operation to create the next generation. Namely, the detailed steps are presented as the following three steps:

Step1. Generate initial population randomly

An initial population was generated randomly with a predetermined size to start fitness evaluation. To assess the fitness of the individual in the current population, an objective function to assess crack detection accuracy is defined as the Eq.(9). Loss and noise are computed based on comparison between the processed image and the target image shown in Fig.6. As a result, the objective function (*f*) has to ensure the accuracy of extracted crack information with the minimum noises and losses as much as possible.

Fig. 5 Optimal parameter adjustment using the genetic algorithm

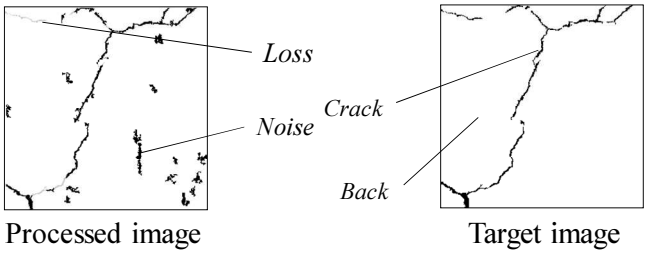

Fig. 6 Target image based fitness evaluation.

Crack and Back are black and white pixels on the Target image, respectively. Meanwhile, Noise is a number of black pixels that appear on the processed image, but it doesn't appear on the target image. Whilst, Loss is a number of pixels that don't appear on the processed image compared with the target image.

$$f = 1 - \sqrt{\frac{f_1^2}{2} + \frac{f_2^2}{2}}, f \in [0\ 1] \qquad (9)$$

$$f_1 = \frac{\text{Loss}}{Crack}; f_2 = \frac{Noise}{Back}$$

Where f_1, f_2 are loss rate and noise rate, respectively. f measures the accuracy of crack detection. f is larger value, the accuracy is higher.

The accuracy and the processing time can be considered as evaluation costs. As the first step, to compare with our previous method, the evaluation cost based on the noise and loss ratios were applied, as shown in the Eq.(9).

Step2. Evolution operation

The evolution operation comprised of selection, crossover, and mutation is repeated until finding best solution. Selection progress is to mimic the natural survival of the creatures. Each string has a corresponded fitness value. The probability of each string to be selected is proportional to its fitness value based on the roultte wheel rotation randomly. The process is repeated for the second parent. Two elite members are kept forward to the next generation.

To improve quality of individual fitness, the crossover operation is used to create two new children from two selected parents with predefined probability. Crossover point is point laid on between 0 to the end of chromosome length. In this study, the single crossover point is selected. The part of the first parent chromosome that runs until the crossover point is spliced with the part of the second parent chromosome that includes, and runs after, the crossover point shown in Fig.5. The whole new generation is selected in this manner.

The mutation of bit strings ensue through bit flips at random positions. The purpose of the mutation operation is to create genotype diversification in the population in order to avoid local optimization leading to finding the best solution.

Mutation point is chosen randomly. However, mutation rate is very small under 1% to avoid collapsing the genetic structure of the current population.

Step3. Stopping criterion

Evaluation of each individual meets the predefined maximum generation, or the best value of the objective function is found.

3. EXPERIMENT

3.1 Sample test

The tunnel lining surface images were captured in various complex environmental conditions. Each inspection image of (3456x4608) pixels with 0.072 mm/pixel resolution was divided into 300x300 pixels to reduce computation time effectively.

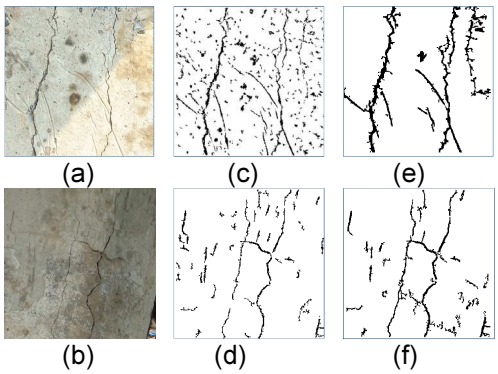

Fig.7 The effectiveness of the dilation and thinning transformation; (a)&(b): Original images; (c)&(d): Proposed method without dilation/thinning has the accuracy *f*=0.8575 & *f*=0.8753, respectively: (e) & (f) : Proposed method with dilation/thinning has the accuracy *f*=0.9542 and *f*=0.9595

This paper used the following equation (10) to estimate the detectable minimum crack width [18].

$$w \geq 0.5 \times fs \times r \qquad (10)$$

Where w is the detectable crack width, fs is the size of the structuring element, and r is the image resolution. Therefore, the detectable minimum crack width of the proposed method would be 0.25 mm because the size of a structuring element is 7x7 pixels and the resolution of the original images in this paper is 0.072 mm/pixel. However, the formula was not verified by experiment in this paper. In the future, the authors will confirm the detectable minimum crack width.

3.2 The dilation and thinning transform experiment

Fig.7 shows the results of the experiment of the proposed method with and without dilation–thinning transform. As a result, without dilation-thinning transform, the accuracy of crack detection result decreases due to noises. Having dilation-thinning transform, the accuracy (*f*) of crack detection is improved significantly from 0.8575 to 0.9542 for Fig.7 (a), and from 0.8753 to 0.9595 for Fig.7 (b).

3.3 Performance evaluation

To validate the effectiveness of crack detection algorithms, the crack detection accuracy of the proposed method (denoted method 1) is compared with the one of our previous method called method 2 [16]. As can be seen in Fig.8, the accuracy value of crack detection of the method 1 is higher than the one of the method 2. However, the crack line of the method 1 is wider than the target image while the crack width of method 2 is similar to the one of the target image. This reason is that the main aim of the method 1 is to remove the noises surrounding the crack line using the dilation-thinning transform. In contrast, the method 2 prefers to reduce the noise laying the crack line. These tendencies depend on image processing techniques in the methods. So far, the average accuracy of the crack detection using methods 1 and 2 are 0.9578 and 0.9202, respectively. It is concluded that application of dilation-thinning transform

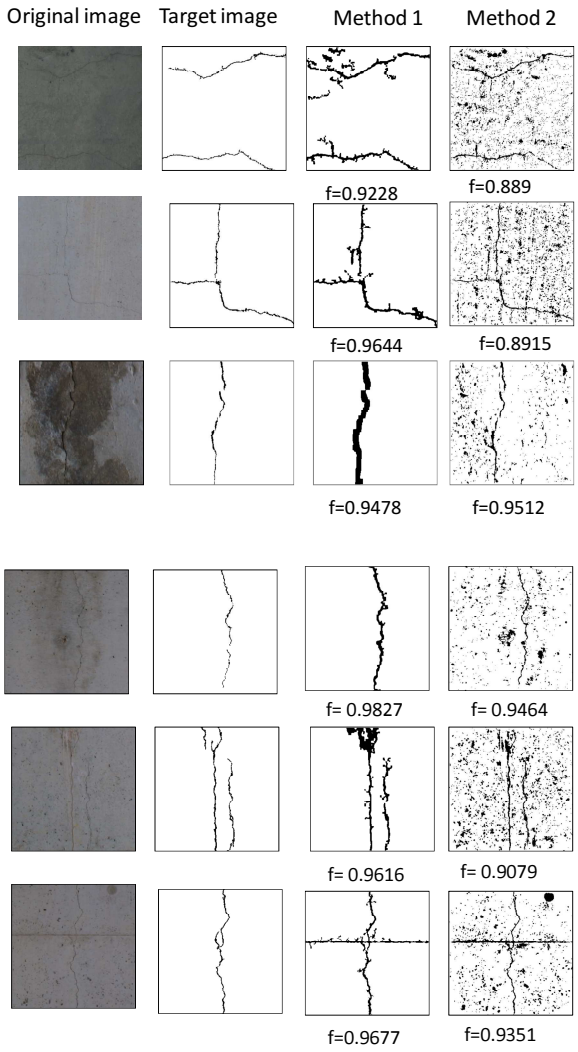

Fig.8 The crack detection results of proposed method and our previous method. The first column is original images. The second column is the target images. The third column is the results of proposed method. The fourth column is the results of method 2.

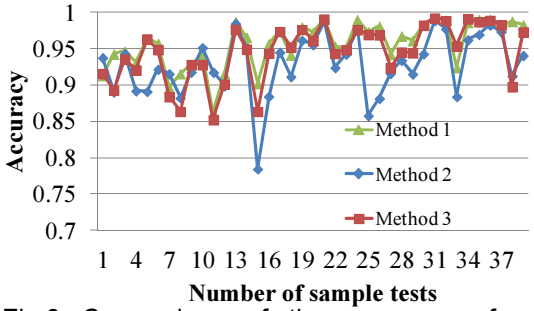

Fig.9 Comparison of the accuracy of crack detection methods

with the optimal size of the structuring element based on GA improves the crack detection results extremely.

Further, Fig.9 shows the results of comparison three methods. Therein, method 3 is the proposed method using Otsu's threshold [19] instead of the global

optimized threshold of the binarization by GA. As can be seen in Fig.9, the vertical axis is the accuracy of crack detection method, and the horizontal axis is number of sample tests included 40 images with various environmental conditions. As a result, the best crack detection accuracy belongs to method 1. The results of method 3 are better than method 2. There are not much difference between method 1 and method 3.
The sample tests in this experiment are not complete. However, they are effective enough to supply a sense of the ideas validated this work.

4. CONCLUSION

The experimental results of various low-contrast surface images of concrete infrastructures under complex brightness conditions demonstrated that the effectiveness of the proposed method. However, the crack width results of the method 1 were larger than the ones of the target image. This reason was that the proposed method 1 prioritized to detect the thin cracks without losing the crack pixels. This method preferred to remove noises surrounding the crack line significantly. Moreover, the tradeoff between the reduction rate of noise surrounding the crack line and the one laying the crack line depended on the type of objective function. This problem would be solved in the future work.

ACKNOWLEDGEMENT

The research is supported by the financial support of JSPS KAKENHI Grant Number 15K0618, and scholarship of Ministry of Construction Vietnam.

REFERENCES

[1] Ito, A., Aoki, Y., and Hashimoto, S. (2002). "Accurate Extraction and Measurement of Fine Cracks fiom Concrete Block Surface Image" In IECON 02 Industrial Electronics Society, IEEE 2002 28th Annual Conference of the IEEE, 2202–2207.

[2] Miyamoto, A., Kono, M., and Bruhwiler, E., (2007). "Automatic crack recognition system for concrete structures using image processing approach", Asian Journal of Information Technology, 6(5), 553–561.

[3] Fujita, Y., Mitani, Y., and Hamamoto,Y., (2006) "A method for crack detection on a concrete structure" ICPR2006: IEEE 18th Int.Conf, on Pattern Recognition, Vol.3, New York, 901-904.

[4] Yu, S., Jang, J., and Han, C., (2007). "Auto inspection system using a mobile robot for detecting concrete cracks in a tunnel" Automation in Construction, 16(3), 255–261.

[5] Ukai, M., (2000), "Development of image processing technique for detection of tunnel wall deformation using continuously scanned image", Quart. Rep. – RTRI 41 (3), 120–126.

[6] Yamaguchi, T., and Hashimoto, S., (2010). "Fast crack detection method for large-size concrete surface images using percolation-based image processing." Machine Vision and Applications, 21(5), 797–809.

[7] Zhu, Z., German, S., and Brilakis, I., (2011). "Visual retrieval of concrete crack properties for automated post-earthquake structural safety evaluation." Automation in Construction, Elsevier B.V., 20(7), 874–883.

[8] Abdel-Qader, I., Abudayyeh, O., Kelly, E., (2003) "Analysis of egde-detection techniques for crack identification in bridges", J. Comput. Civil Eng. 17 (4) 255–263.

[9] Nguyen Kim, C., Kawamura,K., Tarighat, A., Matsumoto, J., and Shiozaki, M., (2016), "Development of semi-automatic crack detection software for concrete structures", 11th fib International PhD Symposium in Civil Engineering.

[10] Chaiyasarn, K., (2011) "Damage Detection and Monitoring for Tunnel Inspection based on Computer Vision", Christ's College, University of Cambridge, UK, Dissertation,.

[11] Kawamura, K., Miyamoto, Nakamura, A. H. , Sato, R.: "Proposal of a crack pattern extraction method from digital images using an interactive genetic algorithm" Proc. Japan Soc. Civ. Eng. Vol.742, 2003, pp. 115-131.

[12] Nishikawa, T., Yoshida, J., Sugiyama, T., Fujino, Y., "Concrete crack detection by multiple sequential image filtering", computer-Aided civil and infrastructure engineering 27, 2012, pp 29-47.K.

[13] Sinha, K.S., Fieguth, P.W, "Automated detection of cracks in buried concrete pipe images", Automation in Construction 15,2006, 58-72.

[14] Jahanshahi, M.R, Masri,S.F., (2012) "Adaptive vision-based crack detection using 3D scene reconstruction for condition assessment of structures", Automation in Construction, 567-576.

[15] Zhang,W., Zhang, Z., (2014) "Automatic Crack Detection and Classification Method for Subway Tunnel Safety Monitoring", Sensors, , 14, 19307-19328.

[16] Nguyen, C., Kawamura., K., Tarighat, A., " A study on seme-automatic concrete cracks detection using interactive genetic algorithm", JCI, vol 38(1), 2061-2066, 2016.

[17] Lam, L., Seong-W.L, and Ching Y.S, "Thinning Methodologies-A Comprehensive Survey," IEEE Transactions on Pattern Analysis and Machine Intelligence, Vol 14, No. 9, September 1992, page 879.

[18] Zhao, L., and Niu, L., (2012) " Study on Key Technique of Image Processing and Automatic Recognition of Tunnel Cracks", ICLEM, 427-433.

[19] Otsu, N., (1979) "A threshold selection method from gray-level histograms", IEEE Trans Syst Man Cybern 9:62-66.